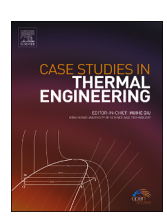
FISEVIER

Contents lists available at ScienceDirect

# Case Studies in Thermal Engineering

journal homepage: www.elsevier.com/locate/csite



# Influence of space conjugate temperature varying non-uniform heat sink/source on hydromagnetic slip water-EG (50:50) nanofluid

Yaqun Niu<sup>a</sup>, M.K. Nayak<sup>b,\*</sup>, S. Yashodha<sup>c</sup>, S. Nazari<sup>d</sup>, A.K Abdul Hakeem<sup>c</sup>, Rifaqat Ali<sup>e</sup>, Syed Zaheer Abbas<sup>f</sup>, Ali J. Chamkha<sup>g</sup>

- <sup>a</sup> Department of Mathematics, Taiyuan University, Taiyuan 030032, Shanxi, China
- <sup>b</sup> Department of Mechanical Engineering, ITER, Siksha 'O' Anusandhan Deemed to Be University, Bhubaneswar, 751030, India
- c Department of Mathematics, Sri Ramakrishna Mission Vidyalaya College of Arts and Science, Coimbatore, 641020, India
- <sup>d</sup> Young Researchers and Elite Club, Islamic Azad University, Tehran, Iran
- <sup>e</sup> Department of Mathematics, Applied College in Mohayil Asir, King Khalid University, Abha, Saudi Arabia
- <sup>f</sup> Faculty of Transport Engineering, University of Pardubice, 53 210 Pardubice, Czech Republic
- g Faculty of Engineering, Kuwait College of Science and Technology, Doha District, Kuwait

#### ARTICLE INFO

Handling Editor: Huihe Qiu

Keywords: MHD Source/sink Vertical cone Heat transfer

#### ABSTRACT

Significant cooling is an essential requirement in the field of aeronautical and bio-medical engineering, nuclear reactor system, solar collectors, and in development of electronic chips etc. Involving rotating conical geometries. In view of this, flow and heat transfer over conical geometries subject to different constraints of motion are highly needed. Implementation of magnetic field subject to flow pattern controls the fluid motion thereby imparting better cooling. Consideration of nanofluid instead of regular fluid yields prominent cooling of the associated surface. Such relevance has motivated the authors to work on magnetohydrodynamics and heat transfer investigation of water-EG (50:50) mixture based  $Al_2O_3$  and  $Fe_3O_4$  past heated and rotating down-pointing upright cone subject to impact of space and temperature varying non-uniform heat source or sink. Numerical solution of dimensionless governing equations is accomplished by implementing Runge-Kutta method. The findings indicate that swirl and axial velocities peter out with rise in magnetic parameter while both exhibit opposite impact in response to slip parameter. Temperature profiles upgrade due to amplification of space and temperature dependent parameters. Skin friction and heat transportation upsurge with growth of solid volume fraction of nanoparticle.

#### 1. Introduction

Customizing the execution of industrial tools in the field of heat transfer (HT) is very challenging one. Early stage of research is mainly aimed using base fluids for HT phenomenon, but later on, to overcome this, Choi and Eastman [1] came up with an innovative type of fluids called nanofluids (NFs), which is a boon in enhancing the thermal conductivity. In recent years significant methods are developed to modify thermal performance of fluids by putting nano sized solid particles like  $Al_2O_3$ , Cu, Ag etc. in fluids, which are poor in HT. Hakeem et al. [2] conducted a comparative study with magnetized/non-magnetized nanoparticles. Soret-Dufour impacts

E-mail address: mkn2122@gmail.com (M.K. Nayak).

<sup>\*</sup> Corresponding author.

on magnetized Casson NF flow across an inclined plane were perused by Lorenzini et al. [3]. They found that the solutal and thermal distributions improve and velocity slows down with Casson parameter. The impact of Brownian movement and thermophoresis on chemically-reacting magnetized Hiemenz stream across a nonlinear expandable plate was investigated by Ibrahim et al. [4]. Impacts of slip on magnetic Casson nanofluid flow over a permeable stretched sheet were perused by Kumar et al. [5]. 3D NF stirring with a non-uniform heat sink/source was studied by Thumma et al. [6]. They discovered that an upsurge in the stretching ratio parameter had an impact on the axial velocity profile. Sheri and Thumma [7] investigated the thermal and solutal effects on natural convection flow when various volume fractions of copper-water nanofluid were present. They discovered that concentration profiles get more emaciated as Schmidt number increase. MHD convective NF flow over a rotating inclined thin layer of iron oxide based on sodium alginate was discussed by Dawar et al. [8]. The effects of magnetohydrodynamics, heat source/sink, and gravity modulation on the movement of a micropolar hybrid NF fluid across an inclined surface were studied by Ali et al. [9]. They found that fluid velocity amplifies with rising Hartmann number but emaciates with growth of micropolar material amount. The works on the related areas were seen in Refs. [10–34].

Fluid flow due to rotating conical geometries has gained importance in the field of aeronautical engineering, cooling nuclear reactor system, solar collectors, and medical field and in development of electronic chips etc. The investigation on free convection (Hering and Grosh [35]), mixed convection (Yih [36]), variable viscosity (Hossain et al. [37]), MHD (Chamkha and Al-Mudhaf [38]), and Soret/Dufour effect (Huang [39]) of nanofluids over rotating cone. The flow of MHD Ellis nanofluids around a spinning cone was perused by Ahmed et al. [40]. They stated that as bioconvection Rayleigh number ups, the temperature and velocity gradients decrease. The flow of water-copper NF and enhancement of HT between vertical concentric cones were studied by Bairi [41]. Their findings demonstrate that heat transmission improves with increasing thermal conductivity ratios, concentrations of nanoparticles, and Rayleigh numbers. The double-diffusive magnetized Jeffrey fluid flow via the disc and cone region was analysed by Khan et al. [42]. They discovered that when the thermic relaxation factor and Prandtl number increase, the thermal distribution slows down. The magnetic Casson liquid considering the impacts of Dufour and Soret because of a revolving cone was analysed by Mustafa et al. [43]. The magnetic parameter reduces the tangential and azimuthal velocities. Natural convective dissipative NF flow via a vertical cone was observed by Ragulkumar et al. [44]. They discovered that the fluid velocity and temperature of NF rise in tandem with increment in viscous dissipation parameter. The works on the related areas were carried out in Refs. [45–48].

The studied literature revealed that many works have carried out regarding the flow and HT of regular fluids or NFs over rotating cone with magnetic field. However, none of them investigated the influences of space and temperature varying heat source/sink on the stream and HT of NFs over rotating cone. The above gap in the existing literature and the relevance of NF flow over conical geometries of industrial importance were the main motivation behind the present investigation. Therefore, the objective of the existing work is to investigate the free convection flow about a vertical spinning cone under the effect of magnetic field, space and temperature varying heat source or sink using water-EG (50:50) mixture as base fluid and  $Al_2O_3$  and  $Fe_3O_4$  as nanoparticles. The novelties of the present study are:

- Introduction of space and temperature varying heat sink or source.
- Consideration of  $Al_2O_3/Fe_3O_4$  + water-EG (50:50) NF as the flow medium over a vertical spinning cone.

#### 2. Modeling

Consider an incompressible, steady, laminar and 2D magnetohydrodynamic flow of  $Al_2O_3/Fe_3O_4 + H_2O-C_2H_6O_2$  (50:50) NF along a rotating down-pointing upright hot cone subjected to magnetic field and space conjugate temperature varying heat source or sink. Cone has angular velocity shown by  $\Omega$  and the flow's local radius is taken as  $r = xsin\gamma$ . Consider u,v,w are respectively velocity elements in x,y and $\theta$  directions. Problem geometry is shown in Fig. 1. Thermophysical properties of  $H_2O-C_2H_6O_2$  (50:50) and  $Al_2O_3/Fe_3O_4$  are mentioned in Table 1.

Using the assumptions mentioned earlier, governing equations would be ([35,38,44,47]):

$$\frac{\partial (ru)}{\partial r} + \frac{\partial (rv)}{\partial v} = 0,\tag{1}$$

$$\rho_{\rm nf} \left( u \frac{\partial u}{\partial x} + v \frac{\partial u}{\partial y} - \frac{w^2}{x} \right) = \mu_{nf} \frac{\partial^2 u}{\partial y^2} + (\rho \beta)_{\rm nf} g \cos \gamma \left( T - T_{\infty} \right) - \sigma_{nf} B_o^2 u, \tag{2}$$

$$\rho_{\rm nf}\left(u\frac{\partial w}{\partial x} + v\frac{\partial w}{\partial y} + \frac{uw}{x}\right) = \mu_{\rm nf}\frac{\partial^2 w}{\partial y^2} - \sigma_{\rm nf}B_{\rm o}^2w,\tag{3}$$

$$\left(\rho C_{p}\right)_{nf}\left(u\frac{\partial T}{\partial x}+v\frac{\partial T}{\partial y}\right)=k_{nf}\frac{\partial^{2}T}{\partial y^{2}}+\underbrace{\frac{k_{nf}u}{xv_{nf}}\left[A^{*}\left(T_{w}-T_{\infty}\right)exp\left(-\frac{y}{L^{2}}\right)+B^{*}\left(T-T_{\infty}\right)\right]}_{space\ and\ temperature\ dependent\ non-uniform\ heat\ source/sink}$$
(4)

Boundary conditions ([38,47]):

$$u = L_1 \frac{\partial u}{\partial y} + L_2 \frac{\partial^2 u}{\partial y^2}, v = 0, w = r\Omega + L_3 \frac{\partial w}{\partial y} + L_4 \frac{\partial^2 w}{\partial y^2}, T = T_w \text{ at } y = 0,$$
(5)

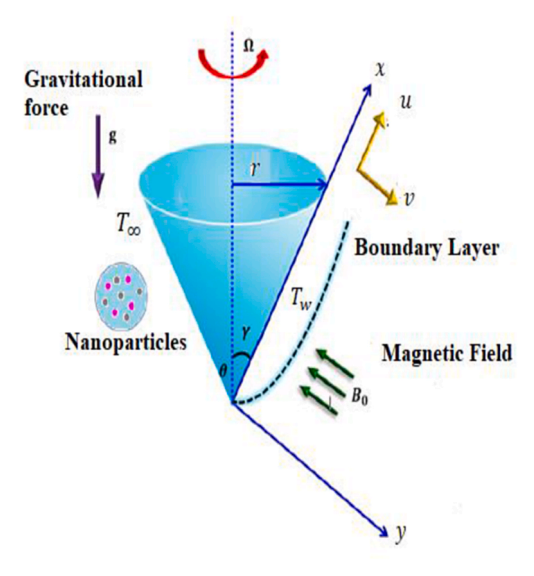


Fig. 1. Flow diagram.

Table 1 Thermal and physical properties of  $\mathbf{H}_2\mathbf{O}$ - $\mathbf{C}_2\mathbf{H}_6\mathbf{O}_2$  (50:50) base fluid and  $\mathbf{A}l_2\mathbf{O}_3/\mathbf{F}\mathbf{e}_3\mathbf{O}_4$  nanoparticles at 300K

	$C_p$	ρ	k	$\beta \times 10^{-5} \left(\frac{1}{K}\right)$	σ	Pr
EG and water (50:50) mixture $(H_20-C_2H_60_2)$ (50:50)	3288	1056	0.425	0.00341	0.00509	29.86
Aluminium oxide. $(Al_2O_3)$	765	3970	40	0.85	$35\!\times\!10^6$	-
Magnetite ( $Fe_3O_4$ )	670	5180	9.7	1.3	$2.5 \times 10^{4}$	-

$$u = 0, v = 0, T = T_{\infty} \text{ as } y \to \infty, \tag{6}$$

Thermophysical models of nanofluid are described in Table 2. Considering the transformation ([38,47]):

$$\mathbf{u} = \frac{1}{2} \Omega \mathbf{x} \sin \gamma \mathbf{F}'(\eta), \mathbf{v} = -(v\Omega \sin \gamma)^{\frac{1}{2}} \mathbf{F}(\eta), \mathbf{w} = \Omega x \sin \gamma G(\eta), = \left(\frac{\Omega \sin \gamma}{v}\right)^{1/2} \mathbf{y}, \tag{7}$$

$$\Theta(y) = \frac{T - T_{\infty}}{T_{w} - T_{\infty}} \text{ where } T_{w} - T_{\infty} = \left(T_{0} - T_{\infty}\right) \frac{x}{L},\tag{8}$$

We have

$$F''' - \left(\frac{F'^2}{2} - FF'' - 2G^2\right) (1 - \phi)^{2.5} (1 - \phi + \phi (\rho_s/\rho_f)) - \frac{\sigma_{nf}}{\sigma_f} (1 - \phi)^{2.5} MF', +2(1 - \phi)^{2.5} (1 - \phi + \phi ((\rho \beta)_s/(\rho \beta)_f)) \lambda \Theta = 0, \tag{9}$$

$$G'' - (1-\phi)^{2.5} (1-\phi + \phi(P_5/P_f)) \left(F'G - FG'\right) - \frac{\sigma_{nf}}{\sigma_f} (1-\phi)^{2.5} MG = 0, \tag{10}$$

Table 2
Thermophysical models of nanofluid.

1 1 3 1 1 1 1 1 1 1 1 1 1 1 1 1 1 1 1 1	
Properties	Nanofluid
Kinematic viscosity	$ u_{ m nf} = \frac{\mu_{ m f}}{(1-\phi)^{2.5}[(1-\phi)\rho_{ m f}+\phi\rho_{ m s}]}$
Density	$\rho_{\rm nf} = (1-\phi)\rho_{\rm f} + \phi\rho_{\rm s}$
Thermal diffusivity	$\alpha_{\rm nf} = \frac{{ m k}_{\rm nf}}{( ho{ m C}_{ m n})_{\rm of}}$
Heat capacitance	$(\rho C_p)_{nf} = (\rho C_p)_f (1 - \phi) + \phi (\rho C_p)_s$
Electrical conductivity	$\frac{\sigma_{ni}}{\sigma_i} = 1 + \frac{3(\sigma-1)\phi}{(\sigma+2)-(\sigma-1)\phi}$ , where $\sigma = \frac{\sigma_s}{\sigma_i}$
Thermal conductivity	$\frac{k_{\rm nf}}{k_{\rm f}} = \frac{(2k_{\rm f} + k_{\rm s}) - 2\phi(k_{\rm f} - k_{\rm s})}{(2k_{\rm f} + k_{\rm s}) + \phi(k_{\rm f} - k_{\rm s})}$
Thermal expansion coefficient	$(\rho\beta)_{\rm nf} = (\rho\beta)_{\rm f}(1-\phi) + \phi(\rho\beta)_{\rm s}$

$$H'' - \frac{k_f}{k_{-6}} Pr \left( 1 - \phi + \phi \left( (\rho C_p)_s J (\rho C_p)_f \right) \right) \left( \frac{1}{2} F' \Theta + \Theta' F \right) + \frac{1}{2} (1 - \phi)^{2.5} \left( 1 - \phi + \phi \left( \rho_s / \rho_f \right) \right) F' \left( A^* \exp \left( -\zeta \right) + B^* \Theta \right) = O, \tag{11}$$

With boundary conditions

$$F' = \gamma_1 F'' + \gamma_2 F''', F = 0, G = 1 + \gamma_3 G' + \gamma_4 G'', \Theta = 1 \text{ at } \eta = 0,$$
(12)

$$F' \to 0, G \to 0, \Theta \to 0 \text{ as } n \to \infty.$$
 (13)

In which  $\lambda = \frac{Gr}{Re^2}$  is mixed convection parameter,  $Re = \frac{L^2\Omega\sin\gamma}{\nu}$  denotes Reynolds number,  $Gr = \frac{g\beta_f\cos\gamma(T_0-T_\infty)L^3}{\nu^2}$  is Grashof number,  $M = \frac{\sigma B_0^2}{\rho\Omega\sin\gamma}$  is magnetic parameter,  $Pr = \frac{\nu}{\alpha}$  is Prandtl number,  $\gamma_1 = L_1\left(\frac{\Omega\sin\gamma}{\nu}\right)^{\frac{1}{2}}$  and  $\gamma_2 = L_2\left(\frac{\Omega\sin\gamma}{\nu}\right)$  are first and second order slip parameter along axial direction,  $\gamma_3 = L_3\left(\frac{\Omega\sin\gamma}{\nu}\right)^{\frac{1}{2}}$  and  $\gamma_4 = L_4\left(\frac{\Omega\sin\gamma}{\nu}\right)$  are first and order slip parameter along swirl direction.

# 3. Local nusselt number (Nu) and skin friction coefficient( $C_f$ )

Skin friction coefficients  $C_f$  and local Nusselt number Nu are defined as

$$C_{\rm f} = \frac{2\tau_{\rm w}}{\rho_{\rm f}(\Omega x \sin \gamma)^2},\tag{14}$$

and 
$$Nu = \frac{Lq_w}{k_f(T_w - T_\infty)}$$
, (15)

Where  $q_w = -k_{nf} \left(\frac{\partial T}{\partial y}\right)_{y=0}$  is surface heat flux and  $\tau_w = \mu_{nf} \left(\frac{\partial u}{\partial y}\right)_{y=0}$  indicates wall shear stress.

The dimensionless forms of  $C_{-}(f)$  & amp; Nu are

$$C_f Re^{1/2} = \left(\frac{\mu_{\rm nf}}{\mu_{\rm f}}\right) F''(0),$$
 (16)

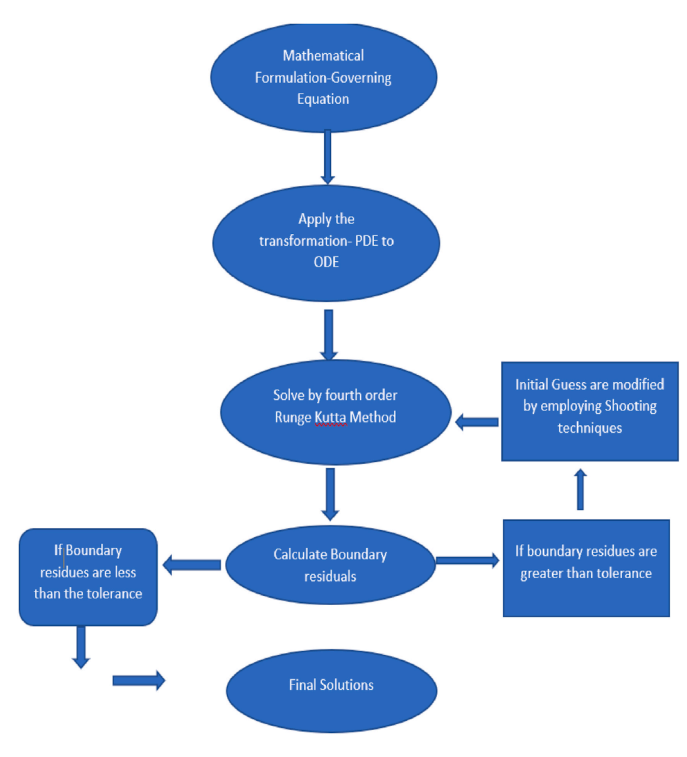
$$NuRe^{-1\backslash/2} = -\left(\frac{k_{nf}}{k_c}\right)\Theta'(0), \tag{17}$$

# 4. Numerical procedure

The BVP may well be solved via fourth order Runge Kutta scheme with shooting techniques. We set  $F = y_1$ ,  $G = y_4$ ,  $\Theta = y_6$ , and hence,

$$\begin{split} y_1' &= y_2, \\ y_2' &= y_3, \\ y_3' &= \left(\frac{F'^2}{2} - FF'' - 2G^2\right) (1 - \varphi)^{2.5} \left(1 - \varphi + \varphi \left(\rho_5/\rho_f\right)\right) + \frac{\sigma_{nf}}{\sigma_f} (1 - \varphi)^{2.5} M \ F' - 2(1 - \varphi)^{2.5} \left(1 - \varphi + \varphi \left((\rho\beta)_5/(\rho\beta)_f\right)\right) \ \lambda \ \Theta, \\ y_4' &= y_5, \\ y_5' &= (1 - \varphi)^{2.5} \left(1 - \varphi + \varphi \left(\rho_5/\rho_f\right)\right) \left(F'G - FG'\right) + \frac{\sigma_{nf}}{\sigma_f} (1 - \varphi)^{2.5} M \ G, \\ y_6' &= y_7, \\ y_7' &= \frac{k_f}{k_{nf}} \Pr \left(1 - \varphi + \varphi \left((\rho C_p)_s/(\rho C_p)_f\right)\right) \left(\frac{1}{2} F'\Theta + \Theta' F\right) - \frac{1}{2} (1 - \varphi)^{2.5} \left(1 - \varphi + \varphi \left(\rho_5/\rho_f\right)\right) F' \left(A^* \exp(-\zeta) + B^*\Theta\right). \end{split}$$

The flow chart for numerical solutions of the developed problem is provided below.



Flow chart for Numerical solutions.

#### 5. Validation

The existing outcomes are compared with that of Chamkha and Al-Mudhaf [12] and Khan et al. [26] and showed excellent agreement (See Tables 3 and 4). Ascending trend of HT rate is visualized with rise in Pr and  $\lambda$ .

# 6. Results and discussion

This part conveys the efficacies of space dependent parameter A\*, spin parameter  $\epsilon$ , magnetic parameter M, nanoparticle volume fraction  $\varphi$ , and temperature dependent parameter B\* on the temperature profile H(y), swirl G(y) and tangential F'(y) velocity profiles in the case of LST is explored. Further, variations of dimensionless  $C_f$  and Nu in response to sundry physical parameters are examined. The values used for parameters in the simulation are:  $\phi = 0.01, M = 1, \lambda = 0.3, A^* = B^* = 1, \gamma_1 = \gamma_2 = \gamma_3 = \gamma_4 = 0.01$ .

Table 3 Comparison of Skin friction coefficient (Chamkha and Al-Mudhaf [12] and Khan et al. [26]).

Pr	λ	Chamkha et al. (2005)	Khan et al. (2020)	Present result
0.7	0	1.0255	1.0256	1.020466
	1	2.2012	2.2017	2.078857
	10	8.5041	8.5044	8.524585
10	0	1.0256	1.0254	1.020465
	1	1.5636	1.5636	1.596575
	10	5.0821	5.0825	5.335744

Table 4
Comparison of Nusselt number (Chamkha and Al-Mudhaf [12] and Khan et al. [26]).

Pr	λ	Chamkha et al. (2005)	Khan et al. (2022)	Present result
0.7	0	0.4299	0.4299	0.428518
	1	0.6120	0.6120	0.612017
	10	1.0097	1.3992	1.017308
10	0	1.4110	1.4113	1.408322
	1	1.5662	1.5663	1.607681
	10	2.3580	2.3582	2.35355

#### 6.1. Influence of M on F'(v), H(v) and G(v)

Fig. 2a reveals the effect of M on F'(y) and G(y) at  $\varphi=0.1$ ,  $\varepsilon=1$ ,  $\Delta=0.1$  and Pr=29.86. When M ameliorates F'(y) and G(y) drop. This is because of the retarding nature of the Lorentz force which is due to the interaction of applied magnetic field and conducting NF thereby reduces the velocity boundary layer thickness. As visualized,  $Al_2O_3$  has higher tangential velocity compared to  $Fe_3O_4$  in M = 0 case. As M increases, magnetic nanoparticle  $Fe_3O_4$  has high tangential velocity than non-magnetic nanoparticle  $Al_2O_3$ . In case of G(y),  $Al_2O_3$  has higher spin velocity than  $Fe_3O_4$ . The influence of M on H(y) for both  $Al_2O_3$ &  $Fe_3O_4$  is portrayed in Fig. 2b. Further, H(y) ameliorates due to rise in M. However, there is subtle variation of H(y) between  $Al_2O_3$ &  $Fe_3O_4$  in appearance/non-appearance of magnetic field.

#### 6.2. Influence of $\varepsilon$ on F'(y), G(y) and H(y)

Fig. 3a depicts that increase in spin parameter  $\varepsilon$  accounts for increase in F'(y) and decrease in G(y). In fact, increase in spin parameter intensifies the movement of the nanoparticles within the NF thereby enhances the fluid motion. It is seen that Fe<sub>3</sub>O<sub>4</sub> has higher tangential velocity than  $Al_2O_3$ . In Fig. 3b it is evident that as spin parameter rises H(y) peters out and  $Al_2O_3$  has high temperature than  $Fe_3O_4$ . This implicates that heat transfer rate ameliorates for enhancement of spin parameter. In fact, rise in spin parameter enables the nanoparticle move faster thereby spend less time near the solid boundary of the cone. As a result, temperature of the NF fluid within BL emaciates.

#### 6.3. Influence of $A^*$ and $B^*$ on H(y)

The effect of  $A^*$  on H(y) is revealed in Fig. 4a. Applying  $A^* > 0$  (heat source) to BL produces energy which helps to increase H(y) while considering heat sink  $(\hat{A}(*) < 0)$  in BL may absorb energy that ensures H(y) to drop. The nanomaterial  $Al_2O_3$  has high temperature compared to  $Fe_3O_4$ . The influence of temperature dependent heat generation or absorption on temperature profile is analysed in Fig. 4b. As  $B^*$  ameliorates, temperature profile uplifts. Further,  $Al_2O_3$  has high temperature compared to  $Fe_3O_4$ .

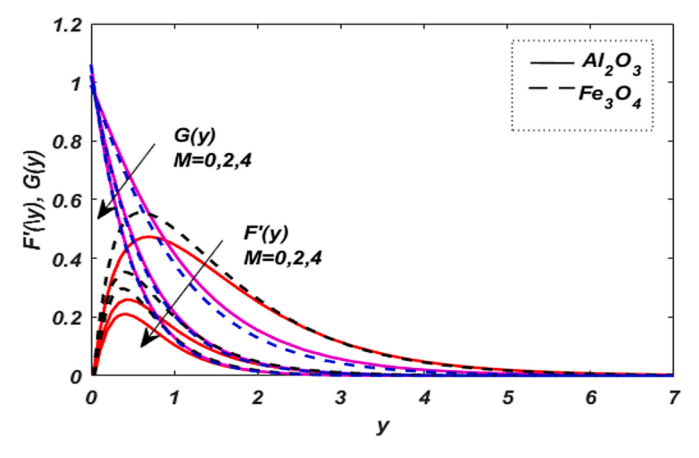


Fig. 2a. Role of M on F'(y) and G(y).

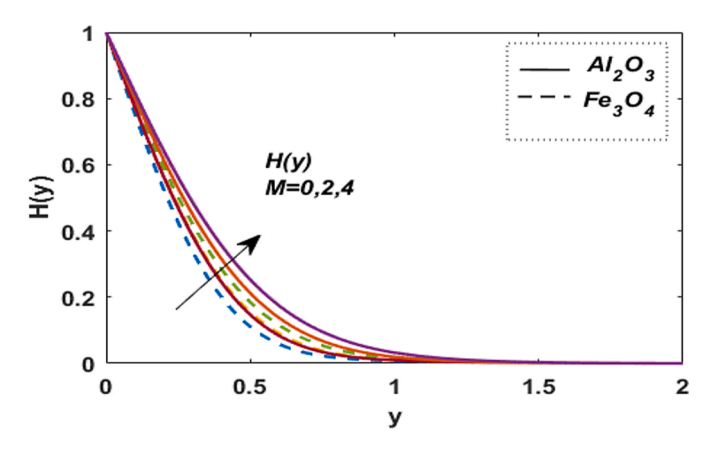


Fig. 2b. Role of M on H(y)

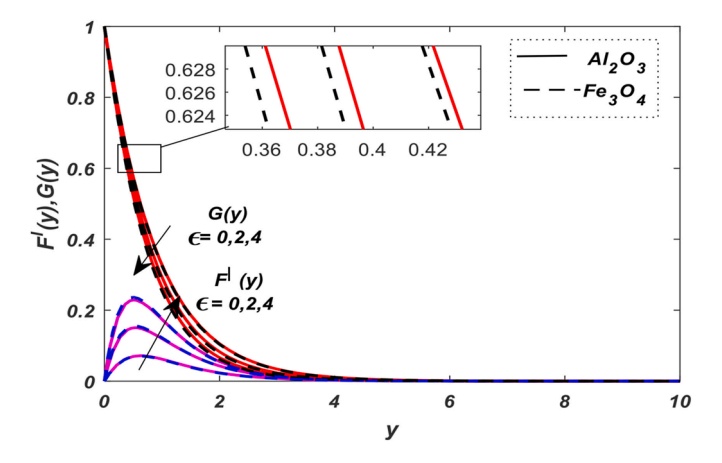
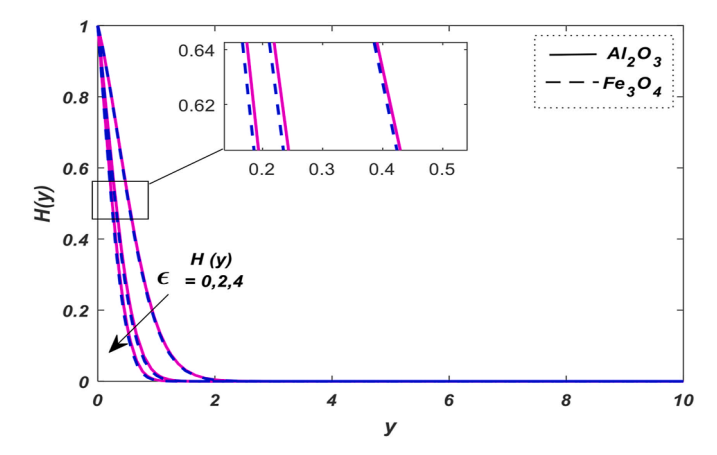


Fig. 3a. Role of  $\varepsilon$  on F'(y) and G(y).



**Fig. 3b.** Role of  $\varepsilon$  on H(y).

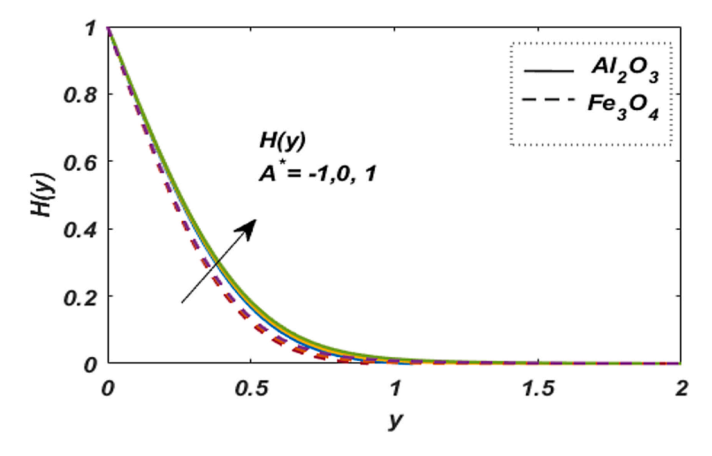


Fig. 4a. Role of  $A^*$  on H(y).

# 6.4. Influence of $\gamma_1, \gamma_2, \gamma_3, \gamma_4$ on F'(y) and H(y)

Fig. 5a, displays the impact of first order slip factor along tangential direction  $\gamma_1$  on  $F(\eta)$ . As  $\gamma_1$  increases there is enhancement in tangential velocity. The F'(y) is higher in the case of  $Fe_3O_4$  than  $Al_2O_3$ . The F'(y) profiles are characterized by overshoots near tangential surface of the cone. This is because  $F(\eta)$  is higher adjacent to solid surface than that of ambient NF. Fig. 5b indicates the effect of  $\gamma_1$  on H(y). As  $\gamma_1$  increases there is drop in temperature. Intensifying slip on the cone's surface reduces the fluid stuck to it. Consequently, fluid temperature peters out. Further,  $Al_2O_3$  has high temperature compared to  $Fe_3O_4$ . As a consequence, the NF with  $Al_2O_3$  as nanoparticle exhibits thicker thermal boundary layer. Fig. 5c displays the role of first order slip parameter along axial direction  $\gamma_2$ 

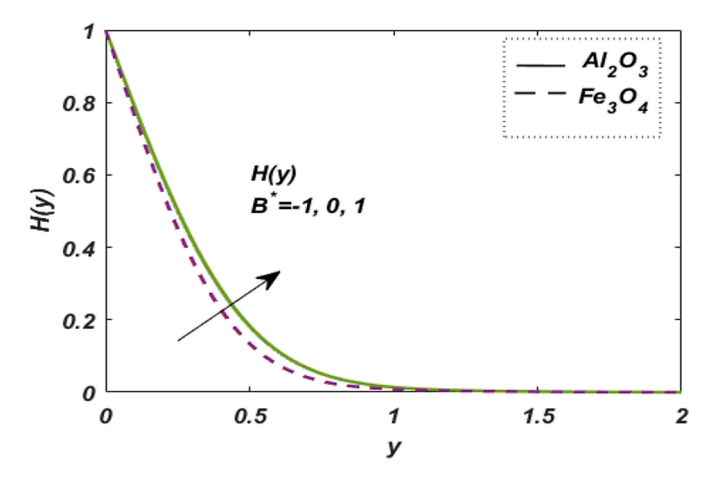
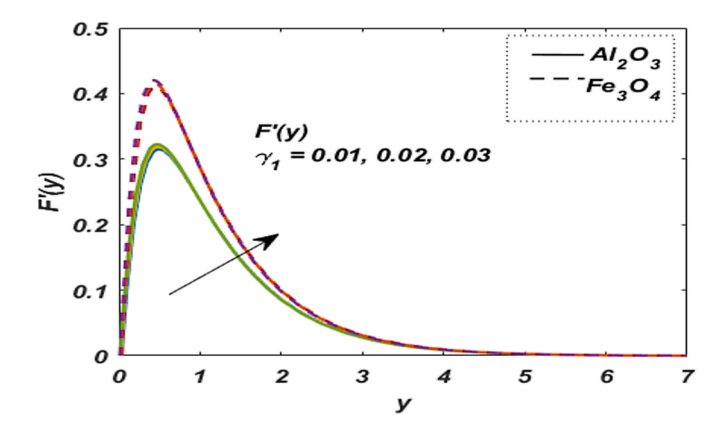
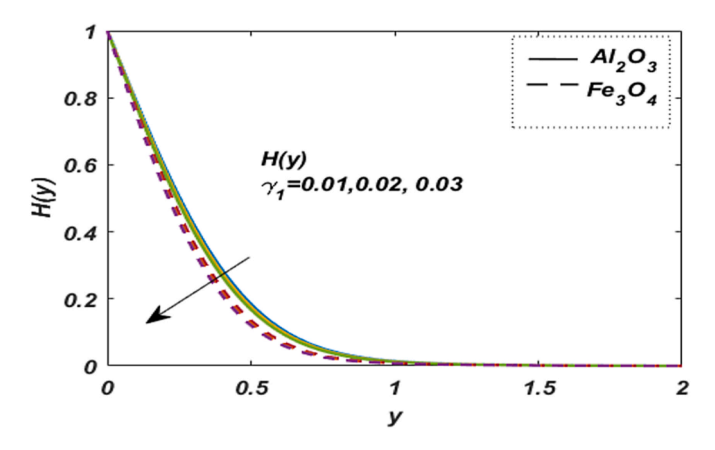


Fig. 4b. Role of  $B^*$  on H(y).



**Fig. 5a.** Role of  $\gamma_1$  on  $F'(\eta)$ .



**Fig. 5b.** Role of  $\gamma_1$  on  $H(\eta)$ .

on velocity profile  $F(\eta)$ . As  $\gamma_2$  rises there is emaciation in  $F(\eta)$  and therefore, velocity boundary layer thickness decays. So rise in slip parameter  $\gamma_2$  generates decelerated flow of NFs in BL region near the surface. Amplifying slip on the cone's surface can lessen the liquid stuck to it which may lead the shear stress to diminish and consequently can impact the movement of the fluid. In addition,  $Fe_3O_4$  possesses higher velocity than that of  $Al_2O_3$ . In case of temperature profile H(y), increase in  $\gamma_2$  leads to intensification of temperature H(y). Further,  $Al_2O_3$  has high temperature than  $Fe_3O_4$  (Fig. 5d). Fig. 5e illustrates that increasing the value of  $\gamma_3$  leads to augmentation of  $F'(\eta)$ . Further,  $F'(\eta)$  of  $Al_2O_3$  nanofluid is lower than that of  $Fe_3O_4$  nanofluid. A similar trend  $\eta$  is visualized for temperature profile  $H(\eta)$  in response to rise in  $\gamma_3$  (Fig. 5f). Fig. 5g and Fig. 5h illustrate that the amplifying  $\gamma_4$  leads to enhancement of  $F'(\eta)$  and enervation in  $H(\eta)$ . In Fig. 5g,  $Al_2O_3$  is dominated by  $Fe_3O_4$ , while opposite trend is visualized in Fig. 5h.

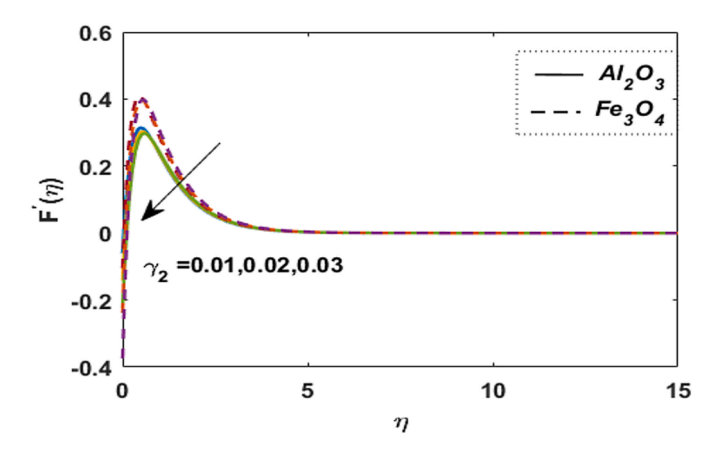


**Fig. 5c.** Role of  $\gamma_2$  on  $F(\eta)$ .

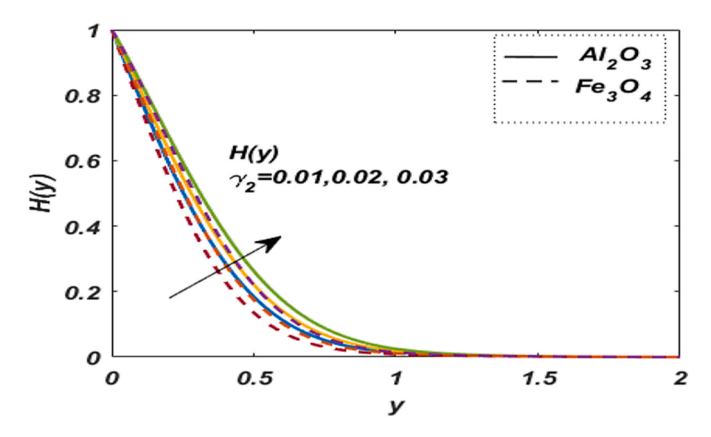


**Fig. 5d.** Role of  $\gamma_2$  on  $H(\eta)$ .

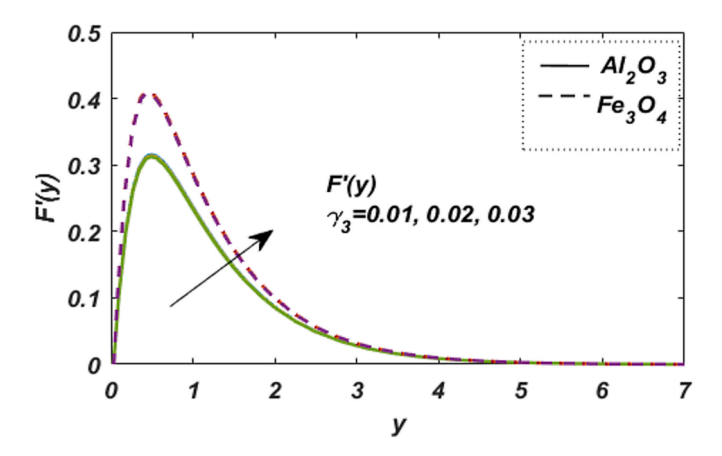


**Fig. 5e.** Role of  $\gamma_3$  on  $F(\eta)$ .

# 6.5. Influence of $\phi$ ,M.A\*,B\* on $C_fRe^{1/2}$ and NuRe<sup>-1/2</sup>

The values of  $C_fRe^{1/2}$  and NuRe<sup>-1/2</sup> for sundry  $\phi$ , M,  $A^*,B^*$  for Al<sub>2</sub>O<sub>3</sub> and Fe<sub>3</sub>O<sub>4</sub> with LST is listed in Table 5. It is noticed that NuRe<sup>-1/2</sup> decreases whereas  $C_fRe^{1/2}$  increases as  $A^*$  and  $B^*$  grow. By comparing nanoparticles  $Al_2O_3$  and  $Fe_3O_4$ ,  $Fe_3O_4$  possessessignificantly higher  $C_fRe^{1/2}$  and NuRe<sup>-1/2</sup> and NuRe<sup>-1/2</sup> and  $C_fRe^{1/2}$  peter out due to strengthening of magnetic field. However, they exhibit reverse trend with increment in volume fraction  $\phi$ .

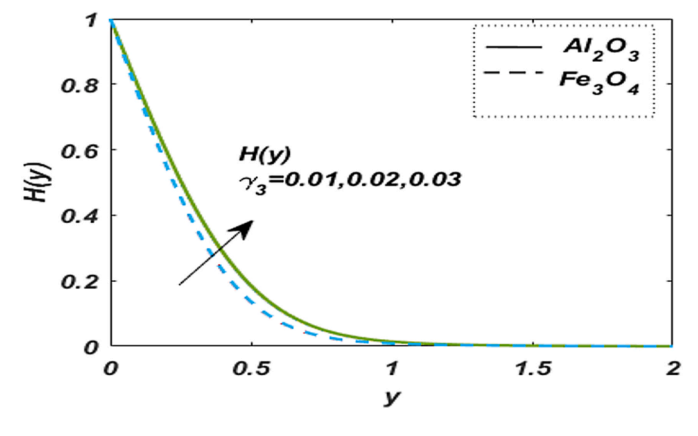


**Fig. 5f.** Role of  $\gamma_3$  on  $H(\eta)$ .

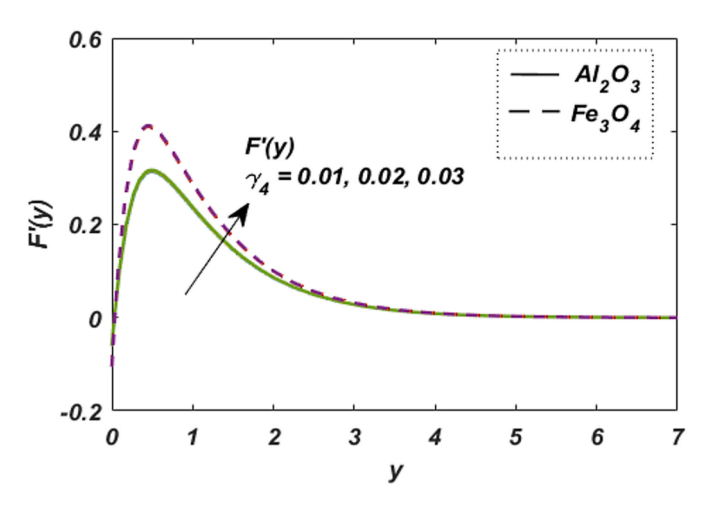


**Fig. 5g.** Role of  $\gamma_4$  on  $F(\eta)$ .

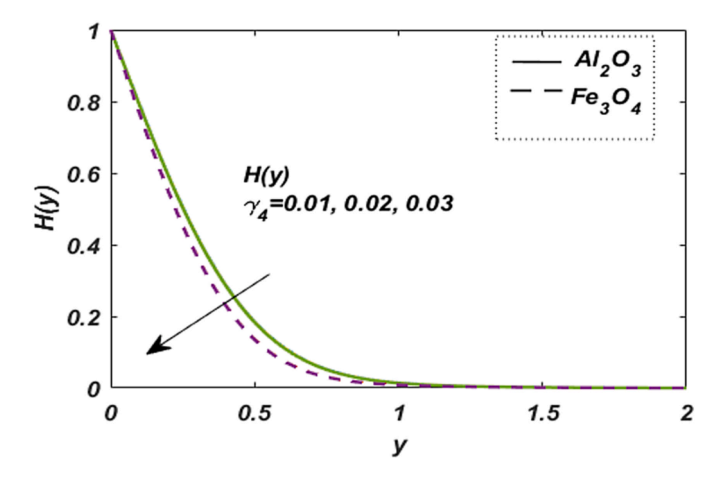


**Fig. 5h.** Role of  $\gamma_4$  on  $H(\eta)$ .

# 7. Conclusions

The existing study deals with the free convective flow and HT of  $Al_2O_3/Fe_3O_4$  + water-EG (50:50) NF over a vertical spinning cone subject to magnetic field, space and temperature varying heat source or sink. The current problem may be utilized in the field of aeronautical engineering, cooling nuclear reactor system, solar collectors, and medical field and in development of electronic chips etc. Employing rotating conical geometries. It is worth to mention the following points from the investigation:

Table 5
The values of .C<sub>4</sub>Re<sup>1/2</sup>,and .NuRe<sup>-1/2</sup>.for sundry .φ.,M, A\*,B\*.for Al<sub>2</sub>O<sub>3</sub> and Fe<sub>3</sub>O<sub>4</sub> with linear surface temperature.

<b>φ</b> Μ		<b>A</b> *	<b>B</b> *	$C_f Re^{1/2}$		Nu <b>Re</b> - 1/2		
				$Al_2O_3$	$Fe_3O_4$	$\mathrm{Al}_2\mathrm{O}_3$	$Fe_3O_4$	
0.01	1	1	1	2.127103	3.237418	2.175797	2.398573	
0.02				3.279087	5.316236	2.445315	2.686296	
0.03				4.373248	7.292505	2.640275	2.87445	
0.01	1	1	1	2.127103	3.237418	2.175797	2.398573	
	2			1.986764	3.089628	2.03683	2.278629	
	3			1.903397	2.997533	1.942622	2.19384	
0.01	1	-2	1	2.048414	3.103143	2.235011	2.44377	
		0		2.098257	3.186411	2.196482	2.413952	
		2		2.159075	3.296437	2.153922	2.382585	
0.01	1	1	-1	2.120062	3.225694	2.195829	2.41859	
			0	2.12356	3.231517	2.185878	2.408656	
			1	2.127103	3.237418	2.175797	2.398573	
0.01	1	1	0.1	1.204577	1.641722	1.864215	2.030396	
			0.5	2.956383	4.673896	2.354564	2.584571	
			1	4.853887	7.987911	2.607726	2.808399	

- Axial velocity F(y) reduces with rise in  $M, \varepsilon, \gamma_2$  while it shows reverse trend with growth of  $\gamma_1$ .
- Swirl velocity G(y) peters out due to amplification of  $M, \varepsilon, \gamma_3$  while it reverses the trend with rise in  $\gamma_4$ .
- Temperature profiles H(y) upgrades with increase in  $M,A^*,B^*,\gamma_2,\gamma_3$  while reverse effect is attained due to rise in  $\varepsilon,\gamma_1,\gamma_4$ .
- As observed, Fe<sub>3</sub>O<sub>4</sub> exhibits higher velocity than that of Al<sub>2</sub>O<sub>3</sub> while Al<sub>2</sub>O<sub>3</sub> possesses higher temperature than that of Fe<sub>3</sub>O<sub>4</sub>.
- The surface viscous drag  $\left(C_f \operatorname{Re}^{\frac{1}{2}}\right)$  and heat transfer rate  $\left(Nu\operatorname{Re}^{-\frac{1}{2}}\right)$  enervate due to strengthening of applied magnetic field while the reverse effect is visualized with amplification of  $\phi$  for both  $Al_2O_3/Fe_3O_4$  + water nanofluids.
- 7.1. Research questions to understand the significance of the results of the current study
- What are the roles of the first and second order slip mechanisms on the behavior of velocities and temperature of magnetic nanofluid flow over rotating conical surfaces.
- Mention the influence of space and temperature varying heat generation/absorption on thermal behavior of magnetic NF flow over rotating conical surfaces.
- In what way the findings of the existing study serve scientifically to the society/industrial world?

#### CRediT authorship contribution statement

Yaqun Niu: Formal analysis, Writing. M.K. Nayak: Methodology, Writing, Simulation, Validation. S. Yashodha: Methodology, Writing, Simulation. S. Nazari: Conceptualization, Methodology, Formal analysis. A.K Abdul Hakeem: Supervision, Conceptualization. Rifaqat Ali: Writing, Formal analysis. Syed Zaheer Abbas: Formal analysis. Ali J. Chamkha: Supervision.

#### Declaration of competing interest

The authors declare that they have no known competing financial interests or personal relationships that could have appeared to influence the work reported in this paper.

#### Acknowledgement

The authors extend their appreciation to the Deanship of Research and Graduate Studies at King Khalid University for funding this work through Large Group Project under grant number RGP2/206/45.

### Data availability

Data will be made available on request.

#### Nomenclature

(u, v, w) velocity elements in the x, y and  $\theta$  directions (ms<sup>-1</sup>)

x coordinate measured along the plane (m) coordinate normal to the plane (m)

MHD magnetohydrodynamic

NF nanofluid HT heat transfer BL boundary layer  $\begin{array}{ll} \rho & \quad \text{Density (Kg m}^{-3}) \\ (\rho C_p) & \quad \text{specific heat capacity} \\ \mu & \quad \text{dynamic viscosity} \\ \sigma & \quad \text{electrical conductivity} \end{array}$ 

k thermal conductivity (Wm<sup>-1</sup>K<sup>-1</sup>) β thermal expansion coefficient (K<sup>-1</sup>)

T temperature (K)

v kinematic viscosity ( $m^2s^{-1}$ )  $\gamma$  half of the vertex angle (rad)  $\Omega$  angular speed of cone ( $rads^{-1}$ ) g acceleration due to gravity ( $ms^{-2}$ )

 $B_0$  magnetic field strength

 $L_1, L_2$  first and second order slip factors along axial direction (m)  $L_3, L_4$  first and second order slip factors along swirl direction (m)

Gr Grashof number
Re Reynolds number

A\* space dependent parameterB\* temperature dependent parameter

Pr Prandtl number

λ mixed convection parameter

 $\varepsilon$  spin parameter M magnetic parameter  $C_f$  skin friction coefficient

 $\gamma_1$ ,  $\gamma_2$  first and second order slip parameters along axial direction  $\gamma_3$ ,  $\gamma_4$  first and second order slip parameters along swirl direction

Nu Nusselt number

 $\phi$  volume fraction of nanomaterial

#### Suffixes

nf nanofluidf base fluids solid nanoparticle

#### References

- S.U. Choi, J.A. Eastman, Enhancing Thermal Conductivity of Fluids with nanoparticles" (No.ANL/MSD/CP-84938; CONF-951135-29), Argonne National Lab. (ANL), Argonne, IL (United States), 1995.
- [2] A.A. Hakeem, S. Saranya, B. Ganga, Comparative study on Newtonian/non-Newtonian base fluids with magnetic/non-magnetic nanoparticles over a flat plate with uniform heat flux, J. Mol. Liq. 230 (2017) 445–452.
- [3] G. Lorenzini, P.V. Kumar, S.M. Ibrahim, A study of soret-dufour effects on MHD radiative Casson nanofluid flow past an inclined surface with chemical reaction, Journal of Advanced Research in Fluid Mechanics and Thermal Sciences 112 (1) (2023) 217–235.
- [4] S.M. Ibrahim, P.V. Kumar, G. Lorenzini, Influence of thermophoresis and brownian motion of nanoparticles on radiative chemically-reacting MHD Hiemenz flow over a nonlinear stretching sheet with heat generation, Fluid Dynam. Mater. Process. 19 (4) (2023).
- [5] P.V. Kumar, C. Sunitha, S.M. Ibrahim, G. Lorenzini, Outlining the slip effects on MHD Casson nanofluid flow over a permeable stretching sheet in the existence of variable wall thickness, J. Eng. Thermophys. 32 (1) (2023) 69–88.
- [6] T. Thumma, S.R. Mishra, M.A. Abbas, M.M. Bhatti, S.I. Abdelsalam, Three-dimensional nanofluid stirring with non-uniform heat source/sink through an elongated sheet, Appl. Math. Comput. 421 (2022) 126927.
- [7] S.R. Sheri, T. Thumma, Heat and mass transfer effects on natural convection flow in the presence of volume fraction for copper-water nanofluid, Journal of nanofluids 5 (2) (2016) 220–230.
- [8] A. Dawar, A. Wakif, T. Thumma, N.A. Shah, Towards a new MHD non-homogeneous convective nanofluid flow model for simulating a rotating inclined thin layer of sodium alginate-based Iron oxide exposed to incident solar energy, Int. Commun. Heat Mass Tran. 130 (2022) 105800.
- [9] B. Ali, S.A. Khan, A.K. Hussein, T. Thumma, S. Hussain, Hybrid nanofluids: significance of gravity modulation, heat source/sink, and magnetohydrodynamic on dynamics of micropolar fluid over an inclined surface via finite element simulation, Appl. Math. Comput. 419 (2022) 126878.
- [10] M.K. Nayak, MHD 3D flow and heat transfer analysis of nanofluid by shrinking surface inspired by thermal radiation and viscous dissipation, Int. J. Mech. Sci. 125 (2017) 185–193.
- [11] S. Shaw, S.S. Samantaray, A. Misra, M.K. Nayak, O.D. Makinde, Hydromagnetic flow and thermal interpretations of Cross hybrid nanofluid influenced by linear, nonlinear and quadratic thermal radiations for any Prandtl number, Int. Commun. Heat Mass Tran. 130 (2022) 105816.
- [12] M.K. Nayak, G.C. Dash, L.P. Singh, Heat and mass transfer effects on MHD viscoelastic fluid over a stretching sheet through porous medium in presence of chemical reaction, Propulsion and Power Research 5 (1) (2016) 70–80.
- [13] S.P. Lakshmi, S. Sobhanapuram, S.R. Devi, S.M. Ibrahim, Investigation of magneto hydrodynamics properties of reiner-philippoff nanofluid with gyrotactic microorganism in a porous medium, CFD Lett. 16 (6) (2024) 1–19.
- [14] P. Roja, S.M. Ibrahim, T.S. Reddy, G. Lorenzini, Chemically radiative MHD flow of a micropolar nanofluid over a stretching/shrinking sheet with a heat source or sink, Fluid Dynam. Mater. Process. 20 (2) (2024).
- [15] T. Thumma, S.N. Pv, Innovations in Eyring–Powell radiative nanofluid flow due to nonlinear stretching sheet with convective heat and mass conditions: numerical study, Aust. J. Mech. Eng. 21 (1) (2023) 221–233.
- [16] M.K. Nayak, Chemical reaction effect on MHD viscoelastic fluid over a stretching sheet through porous medium, Meccanica 51 (2016) 1699-1711.
- [17] M.K. Nayak, N. Karimi, A.J. Chamkha, A.S. Dogonchi, S. El-Sapa, A.M. Galal, Efficacy of diverse structures of wavy baffles on heat transfer amplification of double-diffusive natural convection inside a C-shaped enclosure filled with hybrid nanofluid, Sustain. Energy Technol. Assessments 52 (2022) 102180.
- [18] M.K. Nayak, S. Shaw, H. Waqas, T. Muhammad, Numerical computation for entropy generation in Darcy-Forchheimer transport of hybrid nanofluids with Cattaneo-Christov double-diffusion, Int. J. Numer. Methods Heat Fluid Flow 32 (6) (2022) 1861–1882.

- [19] S Shaw, F Mabood, T Muhammad, MK Nayak, M Alghamdi, Numerical simulation for entropy optimized nonlinear radiative flow of GO-Al2O3 magneto nanomaterials with auto catalysis chemical reaction, Numer. Methods Part. Differ. Equ. 38 (3), 329-358.
- [20] A. Dawar, T. Thumma, S. Islam, Z. Shah, Optimization of response function on hydromagnetic buoyancy-driven rotating flow considering particle diameter and interfacial layer effects: homotopy and sensitivity analysis, Int. Commun. Heat Mass Tran. 144 (2023) 106770.
- [21] R.P. Gowda, R. Naveenkumar, J.K. Madhukesh, B.C. Prasannakumara, R.S.R. Gorla, Theoretical analysis of SWCNT-MWCNT/H 2 O hybrid flow over an upward/downward moving rotating disk, Proc. Inst. Mech. Eng., Part N: Journal of Nanomaterials, Nanoengineering and Nanosystems 235 (3-4) (2021) 97–106.
- [22] T. Thumma, O.A. Beg, S.R. Sheri, Finite element computation of transient dissipative double diffusive magneto-convective nanofluid flow from a rotating vertical porous surface in porous media, Proc. Inst. Mech. Eng., Part N: Journal of Nanomaterials, Nanoengineering and Nanosystems 231 (2) (2017) 89–108.
- [23] M.D. Shamshuddin, S.R. Mishra, T. Thumma, Chemically reacting radiative Casson fluid over an inclined porous plate: a numerical study, in: Numerical Heat Transfer and Fluid Flow: Select Proceedings of NHTFF, 2018, pp. 469–479.
- [24] A.K.A. Hakeem, N. Indumathi, B. Ganga, M.K. Nayak, Comparison of disparate solid volume fraction ratios of hybrid nano fluids flow over a permeable flat surface with aligned magnetic field and Marangoni convection, Scientia Iranica, Transaction F, Nanotechnology 27 (6) (2020) 3367–3380.
- [25] Wenkai Shao, M.K. Nayak, Rifaqat Ali, S. Nazari, Simultaneous numerical examination of thermal and entropy characteristics of Al2O3–H2O nanofluid within a porous diamondshaped container with a \(\perp \)-shaped obstacle, Case Stud. Therm. Eng. 54 (2024) 104059.
- [26] K. Irshad, A.A. Pasha, MK Al Mesfer, M. Danish, M.K. Nayak, A.J. Chamkha, A.M. Galal, Hydrothermal behavior and entropy analysis of double-diffusive nanoencapsulated phase change materials in a porous wavy H-shaped cavity with baffles: effect of thermal parameters, J. Energy Storage 72 (2023) 108250.
- [27] T. Thumma, S.R. Mishra, K. Swain, M. Ijaz Khan, N.M. Khan, Effect of dissipation energy on magnetohydrodynamic 3D stagnation point flow of micropolar nanofluid past a sinusoidal circular cylinder, Waves Random Complex Media 1–26 (2022).
- [28] A. Raza, T. Thumma, S.U. Khan, M. Boujelbene, A. Boudjemline, I.A. Chaudhry, I. Elbadawi, Thermal mechanism of carbon nanotubes with Newtonian heating and slip effects: a Prabhakar fractional model, J. Indian Chem. Soc. 99 (10) (2022) 100731.
- [29] T. Thumma, N.A. Ahammad, K. Swain, I.L. Animasauan, S.R. Mishra, Increasing effects of Coriolis force on the cupric oxide and silver nanoparticles based nanofluid flow when thermal radiation and heat source/sink are significant, Waves Random Complex Media 1–18 (2022).
- [30] M.K. Nayak, A.S. Dogonchi, A. Rahbari, Free convection of Al2O3-water nanofluid inside a hexagonal-shaped enclosure with cold diamond-shaped obstacles and periodic magnetic field, Case Stud. Therm. Eng. 50 (2023) 103429.
- [31] M. Azam, W.A. Khan, M.K. Nayak, Three dimensional flow of Cross nanofluid over bidirectional moving surface in Darcy-Forchheimer medium with Cattaneo-Christov heat flux, Case Stud. Therm. Eng. 49 (2023) 103250.
- [32] W. Shao, M.K. Nayak, S. El-Sapa, A.J. Chamkha, N.A. Shah, A.M. Galal, Entropy optimization of non-Newtonian nanofluid natural convection in an inclined U-shaped domain with a hot tree-like baffle inside and considering exothermic reaction, J. Taiwan Inst. Chem. Eng. 148 (2023) 104990.
- [33] A. Raza, T. Thumma, K. Al-Khaled, S.U. Khan, K. Ghachem, M. Alhadri, L. Kolsi, Prabhakar fractional model for viscous transient fluid with heat and mass transfer and Newtonian heating applications, Waves Random Complex Media 33 (3) (2023) 808–824.
- [34] S.A. Bakr, T. Thumma, S.E. Ahmed, M.A. Mansour, Z. Morsy, Effects of wavy porous fins on the flow, thermal fields, and entropy of the magnetic radiative non-Newtonian nanofluid confined inclined enclosures, Proc. IME E J. Process Mech. Eng. (2022) 09544089211072629.
- [35] R.G. Hering, R.J. Grosh, Laminar free convection from a non-isothermal cone, Int. J. Heat Mass Tran. 5 (11) (1962) 1059-1068.
- [36] K.A. Yih, Mixed convection about a cone in a porous medium: the entire regime, Int. J. Heat Mass Tran. 26 (7) (1999) 1041–1050.
- [37] M.A. Hossain, M.S. Munir, I. Pop, Natural convection with variable viscosity and thermal conductivity from a vertical wavy cone, Int. J. Therm. Sci. 40 (5) (2001) 437–443.
- [38] A.J. Chamkha, A. Al-Mudhaf, Unsteady heat and mass transfer from a rotating vertical cone with a magnetic field and heat generation or absorption effects, Int. J. Therm. Sci. 44 (3) (2005) 267–276.
- [39] C.J. Huang, Effects of internal heat generation and Soret/Dufour on natural convection of non-Newtonian fluids over a vertical permeable cone in a porous medium, J. King Saud Univ. Sci. 30 (1) (2018) 106–111.
- [40] S.E. Ahmed, A.A. Arafa, S.A. Hussein, MHD Ellis nanofluids flow around rotating cone in the presence of motile oxytactic microorganisms, Int. Commun. Heat Mass Tran. 134 (2022) 106056.
- [41] A. Bairi, Porous materials saturated with water-copper nanofluid for heat transfer improvement between vertical concentric cones, Int. Commun. Heat Mass Tran. 126 (2021) 105439.
- [42] A. Khan, T. Gul, I. Ali, H.A.E.W. Khalifa, T. Muhammad, W. Alghamdi, A.A. Shaaban, Thermal examination for double diffusive MHD Jeffrey fluid flow through the space of disc and cone apparatus subject to impact of multiple rotations, Int. J. Heat Fluid Flow 106 (2024) 109295.
- [43] Z. Mustafa, T. Hayat, T. Javed, A. Alsaedi, Unsteady MHD Casson fluid flow with Dufour and Soret's effects due to a rotating cone, Waves Random Complex Media (2023) 1–21. https://doi.org/10.1080/17455030.2023.2188099.
- [44] E. Ragulkumar, P. Sambath, A.J. Chamkha, Natural convective dissipative different nanofluid flow past a vertical cone with heat and mass transfer, Waves Random Complex Media (2023) 1–27, https://doi.org/10.1080/17455030.2023.2226225.
- [45] A. Paul, N. Sarma, B. Patgiri, Mixed convection of shear-thinning hybrid nanofluid flow across a radiative unsteady cone with suction and slip effect, Mater. Today Commun. 37 (2023) 107522.
- [46] M.N. Khan, S. Ahmad, Z. Wang, N.A. Ahammad, M.A. Elkotb, Bioconvective surface-catalyzed Casson hybrid nanofluid flow analysis by using thermodynamics heat transfer law on a vertical cone, Tribol. Int. 188 (2023) 108859.
- [47] A.A. Hakeem, S. Kirusakthika, B. Ganga, M. Ijaz Khan, M.K. Nayak, T. Muhammad, S.U. Khan, Transverse magnetic effects of hybrid nanofluid flow over a vertical rotating cone with Newtonian/non-Newtonian base fluids, Waves Random Complex Media (2021), https://doi.org/10.1080/17455030.2021.1983236.
- [48] AKA Hakeem, S Kirusakthika, B Ganga, M Akilesh, AS Dogonchi, M K Nayak, Hall current and non-linear slip impact on hydro-magneto-thermal hybrid nanofluid flow past a vertical rotating cone with sundry base fluids, Numer. Heat Tran., Part A: Applications, https://doi.org/10.1080/10407782.2023.2222904.